Response to reviewer RC1 comments: se-2020-139-RC1

We thank the anonymous reviewer RC1 for the thoughtful review of our manuscript. The constructive comments helped us to further improve the manuscript.
We edited the manuscript carefully and addressed all comments of reviewer RC1. Please find below the detailed reply to the comments.

All reviewer comments are shown and highlighted as bold text, followed by our answers as indented normal text. Line numbers in our response refer to the tracked revised manuscript.

Please find also attached at the end of this document, the description of our data publication with further details about the seismic catalog reprocessing and its properties. This data publication document will be available with the seismic data catalog through GFZ data services: http://dataservices.gfz-potsdam.de/portal/ as a separate data publication.

General comments of Reviewer RC1

1) The study deals with very interesting data on injection induced seismicity in a unique experiment and gives some valuable results. These are in particular the extended catalog, the focal mechanisms and principal stresses. Providing these data to the scientific community will undoubtly help better understanding the induced seismicity in geothermal projects in hard rocks. However, despite of reasonable language (as I can assess as non-native speaker), the study is not easy to read. This holds e.g. to the parts on catalog methodology and results, which is not easy to understand. One of the reasons is structuring the paper to Methodology and Results sections. It is a good approach in general, but in some cases it breaks the individual topics and makes the paper longer and understanding more difficult. So I recommend to describe only the more sophisticated methods like 2.3, 2.3 and the location part of 2.1.

Authors:
Thank you, we followed your suggestion and focused for the Methodology part only on the location paragraphs of 2.1, on section 2.3 and also on section 2.4 (we assume that this is meant under the second "2.3" in the comment). Nevertheless, we decided not to exclude the first paragraph of the Methodology part (lines 94-101) because it is a short overview of the stimulation and an introduction to the section. To not describe the seismic catalog with too much detail (as mentioned in comment #12 below) and also to avoid repetition with the Results part we deleted the second and third paragraph from the Methodology.

A description of the seismic catalog, especially its reprocessing and its properties, has now been moved to the data publication to keep the manuscript more focused on the seismological study. Finally, we added the following short explanation in lines 102-106:

"The reprocessed seismic catalog with description of its properties is available as separate data publication (see section data availability) and consists of 5,456 events that were detected and located during and after the stimulation (industrial monitoring) and reprocessed in our study. A total of 55,707 smaller events were further detected during and after the stimulation but were not located or processed later on. These were also included in published seismic catalog. For further explanation about the original seismic catalog see Kwiatek et al. (2019)."

We also excluded the entire section 2.2 from the Methodology part, but added the last two sentences of this section as an introduction to section 3.3 in the Results (lines 292-294):

"For the spatial distribution of the seismic moment, the area around the injection well was separated into horizontal bins of 50x50 m. The cumulative seismic moment of all events within each bin was then investigated by disregarding the depth."

To still mention the numbers of absolute and relocated stimulation and post-stimulation events included in the catalog, we modified the following sentence in lines 120-122:

"The enhanced sub-catalog of 5,456 events including 946 post-stimulation events was reprocessed applying a new updated 1D layered velocity model developed from P-wave onset times of calibration shots obtained during a post-injection VSP campaign (Fig. S1, see also data publication)."

Lastly, we also updated the numbers of events included in the catalog in lines 132-138:

"A total of 2,958 reprocessed events were absolute located around the injection well OTN-3 at an epicentral distance of less than 5 km and at depth of 4.5 to 7 km. The hypocenters of these events were included to the reprocessed and published catalog.

To further refine the quality of hypocenter locations, 2,178 from the 2,958 absolute located events with at least 10 P-wave and 4 S-wave picks were selected and the double-difference relocation technique (hypoDD) was applied using the new VSP-derived velocity model (Waldhauser and Ellsworth, 2000)."

We hope that these changes help to improve the understanding and simplify the reading of the paper.

2) I also think that the spectrum of methods applied is too wide with no clear focus. The authors should decide if they present new high quality extensive seismic catalog whose parameters are characterized by a set of suitable (statistical) methods or they present a seismological study including interpretations. The point is that despite the catalog is the most valuable output, it is never characterized by at least Gutenberrg-Richter distribution and similar methods.

Authors:
We decided to keep the description of the new catalog to minimum and shift discussion on its preparation to the separate data publication (please see the data publication document attached at the end of our responses). In consequence, the methodology and processing parts of the manuscript were streamlined, and we focused our analysis on the source mechanisms and mechanisms complexities, so we now believe the focus of the manuscript was sharpened.

3) The authors also spent a lot of effort determining focal mechanisms using quite sophisticated method to get maximum number of mechanisms, they however do not show the whole set of FM and assess their quality.

Authors:
The quality of focal mechanisms was assessed by the root mean square fault plane uncertainties of the estimated focal mechanisms (Hardebeck and Shearer, 2002). We only further investigated focal mechanisms which had uncertainties less or equal 35°, as suggested by Hardebeck and Shearer (2002). Focal mechanisms with associated uncertainties are a part of the data publication, and we indicated this in the text in lines 196-198:

"The final catalog of focal mechanisms includes 191 events with either manually or estimated polarity pattern and is presented with associated uncertainties in the data publication (see section data availability)."

4) I am also not sure about the improved quality of locations in terms of their asymmetric position to the borehole.

Authors:
The asymmetric distribution of hypocenter locations to the borehole is indeed interesting, but we are at the moment very confident that this is the case. This is supported by two independent analyses, one conducted by the main Author and one being a part of new study by Kwiatek et al. (2021).

We identified that the position of the cluster is affected predominantly by the assumed V_P/V_S ratio. Thus, as the positioning of the cluster was vital for the interpretation of the seismicity, we optimized the cluster position using two criteria: 1) the sum of residuals for all events from location procedure should be minimal, and 2) hypocenters of events at the beginning of stimulation should occur in direct vicinity of injection interval. Our analysis, as presented in submitted manuscript, resulted in V_P/V_S ratio optimized to 1.67 (which is not very different from 1.68 assumed in Kwiatek et al., 2019). However, we updated V_P/V_S ratio to 1.71 using new seismic catalog obtained during 2020 stimulation in *OTN-2* well (which is a subject of a pending study of Kwiatek et al., 2021). The new defined constrain was that 3) events from 2020 stimulation should cluster around *OTN-2* well. The final outcome of locations is shown in the Figure below (however, we restrain from presenting 2020 stimulation data in SE manuscript, as this is a part of pending study).

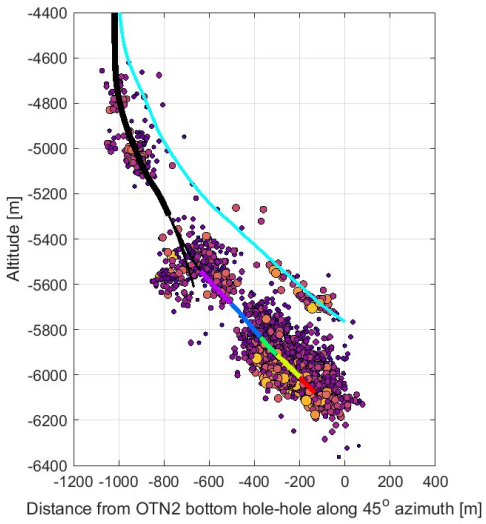

The revised manuscript uses now hypocenters estimated with a V_P/V_S of 1.71. We updated our seismic data catalog.

Using the higher ratio of 1.71, the hypocenters of the 2018 induced events are shifted approximately 300 m upwards in depth. With this shift in depth, the hypocenters are also now more symmetrically located around the injection well, as shown in the revised manuscript (updated Fig. 3a-b). Because of minor changes in takeoff angles, no significant change in focal mechanisms was observed.

We also updated the following sentence in lines 123-126:

"Thus, the V_P/V_S ratio was optimized by a trial-and-error procedure, where we ultimately constrained a V_P/V_S ratio of 1.71 that minimized the cumulative residual errors of all located events, and at the same time kept the first induced events close to corresponding injection well OTN-3."

5) As a result I believe the paper should be restructured according to its main focus - presentation of new data. Details of my comments which should be adressed in a major revision are summarized below.

Authors:
We restructured the manuscript, especially the Methodology and Results parts (for the results, please see the response to comment #12), to focus on the seismological study while keeping the development and properties of the catalog to the minimum. Associated data publication (please see the attached document at the end) contains relevant information on how the catalog was designed and catalog properties.

Particular comments of Reviewer RC1

6) Ln 109-120 (Methodology). The explanation about different subsets of larger and smaller events and their relocation is not very clear. E.g. how many events were above Mw 0.7; were the 3464 events chosen from this subset?; did these events occur during stimulation because you added 321 post-stim events?; did 68 events com from this subset?...

Authors:
With updating our seismic catalog using now a V_P/V_S = 1.71, we also simplified the selection of events used for reprocessing, especially not distinguishing between subsets of larger and smaller events anymore. The reprocessing steps and details about the seismic catalog and its statistical properties are now part of the data publication.

7) Ln 172 - 176. Please explain the SVD application in more detail. The point is that SVD is usually used to find a common pattern in a data set. For this you would need more polarity patterns for each event that just one, which you have as a result of cross correlation. The next question is whether the polarity matrix (eq. 2) shows the polarity fit between the target and template events as indicated on Ln 171 or the fit of polarities themselves. In the first case, it could not be used for calculating focal mechanisms.

Authors:
Indeed, the SVD is usually used to find a common pattern in a data set and this is also the reason why we applied the SVD. The method of Shelly et al. (2016) is a well-established approach were the SVD is applied to extract a common polarity signal from

a matrix that contains the obtained relative polarities between each target events and all template events, considering each station and phase (in our case only P-phase) separately.

For each station, the left singular vector is obtained by applying the SVD to the above mentioned matrix. This vector provides a means of estimating the most consistent set of polarities (sign of the elements) for each target event and station (Shelly et al., 2016).

In our manuscript, the left singular vectors of all stations are presented in the columns of the matrix in equation 2. Therefore, only the most reasonable polarity for each target event and each station is presented in equation 2 as a best fit of many relative polarities derived from cross-correlation between this target event and many templates. Thus, the best fit for each target event still shows a polarity ambiguity. This sign ambiguity of polarities can only be resolved later on when considering the manually picked polarities of some target events.

We restrain from describing the methodology in manuscript in details, as this is a subject of Shelly et al. (2016) where the method is described in details in step-by-step fashion.

We added the following sentence to the manuscript in lines 180-181:

"For each station k, the vectors containing relative polarity estimates between one target event i and all templates j were gathered in a i-by-j matrix."

We further rewrote the following sentence in lines 182-185:

"A Singular Value Decomposition (SVD) was applied to the relative estimated polarity matrix of each station k to extract the strongest common signal of any target event obtained by the first left singular vector of the SVD (Shelly et al., 2016; Rubinstein and Ellsworth, 2010)."

8) Ln 178. The way you reduced the polarity ambiguity is not clear; by considering manually picked events one can verify the automatic picks, I believe.

Authors:
This is precisely what we have performed. Manually picked events and their "true" polarities were used to resolve the ambiguity of SVD-derived polarities for all events at each station, separately. If the SVD-derived polarities has the same sign as the manually picked polarities for one station, than all automatically derived polarities of the other events should also have the right polarities for this particular station due to the first singular vector of the SVD.

We updated the following part of the manuscript (lines 190-192):

"For each station, the SVD-derived polarities of these events were compared with manually picked polarities to investigate whether the polarities have similar or opposite signs. In case of same polarities, the SVD-derived polarities of other events should also show the right sign for the particular stations."

9) Ln 185. The final sentence mentioning the resulting reverse faulting fits rather to the Results than Methodology section.

Authors:
Yes, we agree. We deleted this sentence at the end of our Methodology section.

10) Ln 195. Please argue for using this distance metrics - what is the reason for 1.5 in the denominator? And which type of cluster analysis did you use? What is the difference to the published method of moment tensor clustering of Cesca (2014)?

Authors:
The choice of 1.5 is only to scale the value to range 0-1 (as the Kagan rotation angle θ ranges 0°-120°, our distance metrics PR_{ij} scale from 0 to 1). The cosine was used to rescale Kagan rotation angles and to emphasize large differences in θ. We found for our dataset that this choice does not influence the discussed clustering outcome (i.e. one could use distance metrics based on the Kagan angle θ alone).

As stated in the manuscript, we used well-established hierarchical cluster analysis with distance measured using average distance (Unweighted average distance, UPGMA) and Euclidean distance metrics. The selection of particular distance metrics between clusters was made objectively using the one with highest value of the cophenetic correlation coefficient. Cesca et al. (2014) applied a density-based clustering technique *DBSCAN* (Ester et. al, 1996). Clusters can be identified as densely populated "areas" with a much higher number of points than outside of a presumable cluster. Cesca's approach is more general, as it can be used for non-DC sources. However, in case of pure DC moment tensors, a distance metric based on the Kagan angle alone is used by Cesca et al. (2014), which is comparable to our case.

11) Ln 209-216 (Results). I think that the VSP based model deserves more attention. The present way is not appropriate - to show the model as a result without any more details. If it is considered as a result of this study, the data, methods and results should be shown. In the opposite case, the VSP model can be cited from a different study or as a personal communication from its author.

Authors:
Following Reviewer suggestion, we separated detailed description on catalog development from mechanism complexity analysis. We added details about the VSP velocity model build-up to the data publication. In manuscript we switched Fig. 1 with Fig. S1, as suggested in comment #20. We also added the following sentences to the caption of the new Fig. S1:

"The VSP-derived velocity model shows a velocity inversion between 3 and 6 km depth. Below this velocity inversion, a constant velocity of 6 km s^{-1} is suggested from sonic logs which were used for velocity estimation between 5.1 km and 6.4 km depth."

12) Ln 218-… The description of seismic catalog update appears too detailed and technical and overlaps with the similar section in Methodology. Please consider unifying, making it more clear and concise. Another point concerning locations is the (mis)fit of the hypocenters with the borehole trace. In the depth sections of Fig. 3 it appears that most hypocenters lie below the borehole trace, which is rather unlikely. Please compare e.g. Fig. 3 in Kwiatek et al (2019) where the hypocenters occur almost symmetrically around the borehole.

Authors:
We shortened and restructured the entire section "Seismic catalog update" in the Results part to make it more unified with the Methodology part. A description of the seismic catalog and its reprocessing has now been moved to the data publication. We kept the discussion related to post-stimulation events, as these were not analyzed yet by Kwiatek et al. (2019) or by Hillers et al. (2020).

As mentioned in the response of comment #4 above, by using the updated catalog with a V_P/V_S ratio of 1.71, the hypocenters are now more symmetrically located around the borehole trace (Fig. 3b) and no longer below as it was the case using a V_P/V_S ratio of 1.67.

13) Ln 364. It is interesting that the post-stimulation seismicity does not show any systematic migration. This observation should be supported by a sort of distance-time or coordinate-time plot. In fact, even the existing papers of Kwiatek and Hillers on the Helsinki stimulation do not show such data.

Authors:
Thank you for this comment. We have produced a distance-time plot for the entire stimulation including all separate phases. For each event we took the shortest distance to the open-hole section of the injection well. For phases 1 and 2 we find relative fast migration to roughly 200 m to the well. Starting with phase 3 some events indicate migration out to 400 m distance to the well, but not further. This holds for the post-stimulation phase. The diagram is added to the data publication.

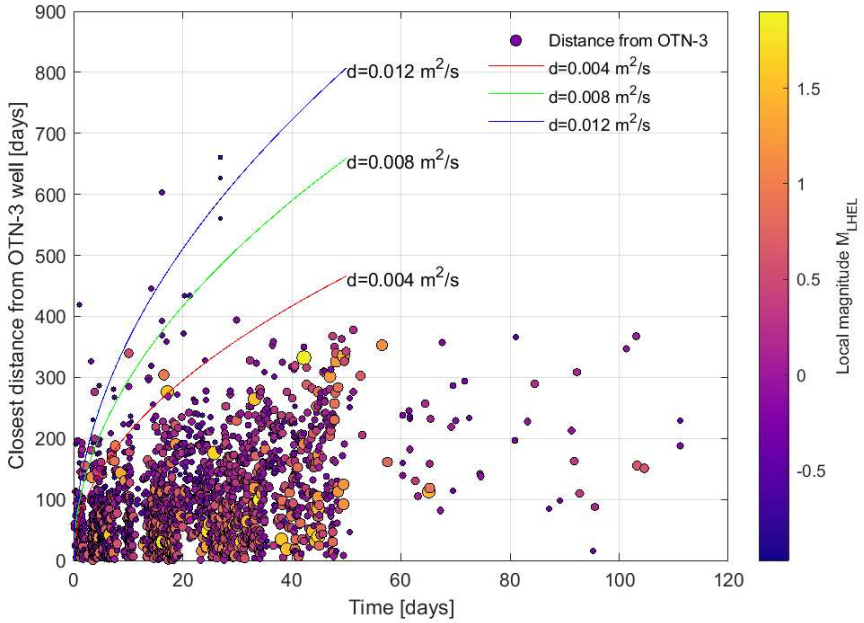

14) Ln 381. To see the events at perimeter these should be shown on top of the others, e.g. in grey.

Authors:
We updated Fig. S4 (in the revised manuscript S3) by plotting the events with $M_W \geq 1$ which occurred during the stimulation in dark grey on top of all relocated events (light

grey) to highlight the narrow zone. We further color-coded events with $M_W \geq 1$ which occurred after the end of stimulation in orange to indicate that these events are located at the perimeters of the narrow zone.

We also added to the caption of this Figure the following sentence:

"Events with $M_W \geq 1$ that occurred during and after the stimulation are color-coded as dark grey and orange, respectively."

15) Ln 393. Please argue for the highest expected pore pressure perturbation at the bottom of the permeable zone.

Authors:
(see also reply to comment #16). The largest pore pressure perturbation is simply expected to be at or close to the well and will progressively decrease with increasing distance. Updated seismic catalog shifted events to shallower depths so they are not significantly deeper than the bottom-hole of injection well *OTN-3*. Thus, the highest seismicity activity and largest seismic events are not anymore at the "bottom of the permeable zone", but are correlated to the bottom-hole of the injection well *OTN-3*. It is expected that this area is characterized by highest pore pressure perturbation, as this is where injection was performed in stages 1-3. Attached here is the figure from data publication showing relation between magnitude and depth.

We replaced "bottom" with "deepest" zone in the referred sentence, pointing out to the fact that largest events occur in the bottom cluster.

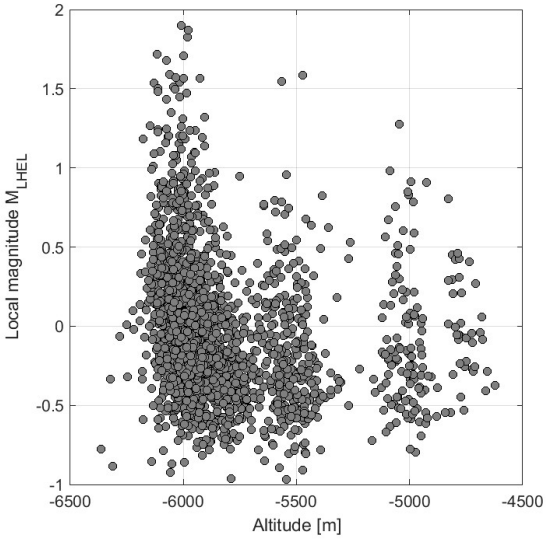

16) Ln 400. The depthward migration is not visible in Fig. 3. And further, it is very unlikely that water would flow down in the expected lithostatic conditions of the rock formation where no open fractures are expected. On the contrary, water tends to flow up due to the buyoancy effect cause by the difference in density of water and rock.

Authors:
We agree with the reviewer that such behavior is quite unexpected, although it is observed in some highly fractured reservoirs (see e.g. Kwiatek et al., 2015, Kwiatek et al., 2018). However, the updated seismic catalog with new V_P/V_S ratio effectively

shifted all events to the shallower depths, rendering original comment on depth migration doubtful. It is still visible that in later stages the seismicity in the bottom cluster tends to locate at larger depths (see previous figure), but the depth of later events is not significantly exceeding the depth of bottom hole of *OTN-3*. This restrained us from suggesting that water flows down, and we suggest that occurrence of seismicity is simply related to pore pressure perturbation that is stronger around the bottom part of injection well *OTN-3*.

17) Ln 442. In the Summary, the authors mention seismic catalog as a result of the study provided to the community. This sounds great, however I would welcome to see some quality analysis of the catalog, at least to show the Gutenberg-Richter distribution distinguishing the original catalog, the newly detected and newly located events.

Authors:
We include the description of the seismic catalog and their properties to the data publication. Besides of providing details about the catalog reprocessing in the data publication, we include there statistical and spatio-temporal properties of developed catalog.

18) Ln 449. The statement "The temporal behavior of the post-stimulation seismic moment release until bleed-off is still similar to the moment release observed during individual stimulation phases" sounds a bit vague.

Authors:
We rewrote the sentence in the Summary and conclusions part:

"Until shortly after the bleed-off, the increase in the cumulative moment release of the post-stimulation seismicity with time is comparable with the slope of the CM_0 during individual stimulation phases but substantially less afterwards. This is especially observed for the seismicity of the deepest hypocenter cluster."

19) Ln 474-476. According to the unclear description of some parts I am not sure if all of the coauthors did really contribute to the manuscript (by e.g. the manuscript correction indicated in the Author contribution section).

Authors:
We state the Author contribution as follows:

"M.L.: data reduction, analysis and results interpretation, draft version of the manuscript, and associated data publication. G.K. and P.M.-G.: data analysis, results interpretation, and manuscript correction. M.B., G.D., and P.H.: results interpretation and manuscript correction. T.S.: project management, drilling and stimulation program development and managing, and manuscript correction."

Comments of reviewer RC1 to the Figures

20) Fig S1. should be included as Fig. 1; this is much more informative than the present Fig. 1 which could be moved to Supplements.

Authors:
We swapped Fig. S1 and Fig. 1.

21) Fig. S2 overlaps with Fig. 2 and using different time scale (absolute vs. relative) makes it different to compare. Why not combining Fig.S2 and Fig.2 in a single plot?

Authors:
Thank you for this suggestion, we combined both Figures to a new Fig. 2 using an absolute time scale. We therefore updated the following sentences in lines 237-239 in the manuscript:

"*The moment magnitudes of the absolute located and relocated seismicity is plotted with time during and after shut-in as grey and orange dots in Fig. 2. The five different stimulation phases (P1-P5) performed in 2018 are also shown in Fig. 2 in combination with the wellhead pressure and seismic event rate.*"

22) Fig. 2 is missing reference in the text. The caption does not explain the meaning of time - from which moment the days are counted? It is also not clear why you do not show also the time period during the stimulation as indicated in the manuscript title and also shown in Fig. 3.

Authors:
Thank you for mentioning the missing reference of Fig. 2. With combining Fig. 2 and Fig. S2 to a new Fig. 2 in the revised manuscript, the reference for Fig. 2 is now mentioned in line 238. For the updated Fig. 2, absolute times (in days) are now used for a better understanding.

Initially we wanted to keep the focus on the post-stimulation seismicity in the original Fig. 2 because this is mainly the new data and not analyzed by Kwiatek et al. (2019) or Hillers et al. (2020) and therefore, the time period during stimulation was not shown. However, the suggestion of combining Fig. 2 and Fig. S2 is a good idea and thus the seismicity and time period during the stimulation is now also presented.
For the updated Fig. 2, we rewrote the caption as followed:

"Stimulation protocol with moment magnitudes of induced seismicity during stimulation phases P1-P5 and post-stimulation time period. The magnitudes of absolute located and relocated events are shown as grey and orange dots, respectively. The green solid line presents the wellhead pressure during the stimulation. The seismic event rate per day is shown by the solid blue line."

23) Fig. 3: The caption should be better specified; e.g. mentioning the name OTN3 of the borehole is missing and the legend does not explain the colored bands along the borehole trace. Are these the stimulated sections and should their color correspond (at the moment it does not) to the colors of hypocenters?

Authors:
We specified the caption by adding the name of the injection well *OTN-3* and explaining the color bands along the borehole trace of *OTN-3*.

We apologize for the confusion about the colored bands along the borehole trace. Unfortunately, the colors along *OTN-3* were wrongly plotted in Fig. 3. We updated the colors which are now corresponding to the colors of the five stimulation stages.

For a better visibility, we also changed the color of the stimulation phase P5 hypocenters to a darker yellow.

24) Fig. 4 and 5: the yellow line is hardly visible.

Authors:
We changed the color to a darker yellow in both Figures.

25) Fig. 5: The three CM0 plots could be better shown with common Y axis, which would spare space and make them more legible, also a single legend would then suffice.

Authors:
Thank you for this suggestion. We updated the Figure using one common y-axis and one legend for all three subplots now.

26) Fig. 9: The black stress component are not visible enough, consider using different color.

Authors:
We now use white as color for the stress component marker symbols and the marker text.

We updated the sentence in the caption of Fig. 9:

"White upward and downward pointing triangle represent maximum and minimum principal stress axes σ_1 and σ_3, respectively."

27) Fig. 10: Please indicate in the caption that the stress ratio R 0.53 determined in the stress inversion is used. And shift the Px markers a bit to the right, these are very hardly visible now.

Authors:
We added the following sentence to the caption of Fig. 10:

"A stress ratio of R = 0.53 was used for stress inversion."

For a better visibility, we also shifted the text of the P1 and P2 markers a bit further outside of each marker symbol.

References not used in the manuscript

Cesca, S., Ali, S., and Dahm, T.: Seismicity monitoring by cluster analysis of moment tensors, Geophysical Journal International, 196, https://doi.org/10.1093/gji/ggt492, 2014.

Kwiatek, G., Martínez-Garzón, P., Plenkers, K., Leonhardt, M., Zang, A., Specht, S., Dresen, G., and Bohnhoff, M.: Insights into complex subdecimeter fracturing processes occurring during a water injection experiment at depth in Äspö Hard Rock Laboratory, Sweden, Journal of Geophysical Research: Solid Earth, https://doi.org/10.1029/2017JB014715, 2018.

Data publication related to

"Seismicity during and after stimulation of a 6.1 km deep Enhanced Geothermal System in Helsinki, Finland"

Maria Leonhardt, Grzegorz Kwiatek, Patricia Martínez-Garzón, Pekka Heikkinen

1. Structure of seismic catalog file

Column 1:

ID number of event

If events were detected but not located, the ID is 0.

Column 2:

Datenumber (integer part = day since year 0)

Column 3-8:

Year, month, day, hour, minute, second

Column 9:

Local "Helsinki" magnitude M_{LHEL}

Column 10:

Moment magnitude M_W

Column 11-13:

Easting (m), northing (m), altitude (m) of absolute location

Column 14-16:

Easting (m), northing (m), altitude (m) of relocation

Column 17-19:

Strike, dip, rake of preferred nodal plane from estimated focal mechanisms

Column 20:

Root mean square fault plane uncertainties of estimated focal mechanisms

For further details about the reprocessing of the catalog and its properties, please see section 2 and 3 below.

2. Seismic catalog development

The original seismic catalog created during stimulation campaign has been reprocessed by Kwiatek et al. (2019), and included 6,150 located and ~54,000 detected earthquakes.

In first step, this catalog was extended in time to cover the post-stimulation period of 63 days. In the following, we selected best quality 5,456 events that were located during and after the stimulation, and reprocessed them in our study, as discussed in details below. The original catalog of detections was reviewed as well, resulting in 55,707 smaller events detected during and after the stimulation. Thus the total seismic catalog presented in this data publication contains 61,163 earthquakes in the period of 112 days that occurred in the vicinity of the *OTN-3* well. In the following sections we present the development of seismic catalog.

2.1 Seismic network

Following Kwiatek et al., (2019), the real-time telemetered network monitoring the stimulation campaign was composed of 24 borehole seismographs, fabricated, installed, and operated by Advanced Seismic Instrumentation and Research (www.asirseismic.com). The 12-level borehole array of three-component 15-Hz natural frequency Geospace OMNI-2400 geophones was sampled at 2 kHz and placed at depths of 1.95 to 2.37 km in the *OTN-2* well. Additional 12-station three-component f_N = 4.5 Hz Sunfull PSH geophones sampled at 500 Hz were installed in 0.30- to 1.15-km-deep wells. These surrounded the project site at 0.6- to 8.2-km epicentral distances. These two networks were operating months before the start of stimulation with no event detected in the vicinity of *OTN-3* injection well. Data from these 24 sensors were used in processing of seismic data forming the data publication.

2.2 Detection catalog

We followed the same approach as presented in Kwiatek et al. (2019). P-wave arrivals unused in locations, but detected using the array located in *OTN-2* well, were further analyzed. Assuming that a small event that is detected solely at the *OTN-2* array must occur in its immediate vicinity, we placed a hypothetical seismic source at the bottom of *OTN-3* where the injection took place. We then calculated travel times of P-waves to the sensors forming the *OTN-2* array, obtaining a particular pattern (offset) of expected P-wave arrivals at these stations. We then scanned the catalog of unused *OTN-2* P-wave arrivals for this particular pattern, and each matching set of detections was attributed to an event occurring in the vicinity of the *OTN-3* well. The magnitude (see section 2.5) was calculated assuming that the event occurred at the bottom of the *OTN-3* injection well. This procedure allowed us to enhance the catalog by 55,707 earthquakes.

2.3 VSP-based velocity model

In original study of Kwiatek et al. (2019), the 1D velocity model based on velocity logs was used. In the study of Leonhardt et al. (2020), the new velocity model was developed from P-wave onset times of calibration shots obtained during a post-injection Vertical Seismic Profiling (VSP) campaign.

The VSP campaign was performed in October 2018 after the end of the stimulation. Overall, 47 calibration shots were performed at 7 shot points located around the injection well *OTN-3* with a maximum distance of less than 8 km. Shot points were prepared with explosives in holes up to 40 m depth. The VSP campaign was monitored by a

17-level vertical chain with 3-components geophones located in the injection well *OTN-3* in a depth between 2.5 km and 4.5 km. In addition, the 12-level vertical geophone chain, used for the stimulation, was also monitoring the VSP shots to cover the depth above 2.5 km.

The 1D velocity model used in Leonhardt et al. (2020) was developed from the data of VSP shot performed close to the OTRA station. This secured that wave propagation ray was nearly vertical between the shot location and seismic arrays. This allowed us to convert travel-path velocities calculated at different sensors forming the array along the *OTN-3* well to interval velocities of the 1D velocity model. For the depths below 4.5 km which was not covered by seismic rays of VSP shots we used information from sonic logs, available depth between 5.1 km and 6.4 km. The velocity model is presented in Fig. 1. Due to a low Signal-to-Noise (S/N) ratio of the VSP data, the S-wave arrival times could not be determined.

The 1D VSP-derived velocity model shows a velocity inversion between 3 and 6 km depth (Fig. 1). The maximum P-wave velocity is 0.15 km s^{-1} larger than the maximum velocity modelled by Kwiatek et al. (2019) where a constant velocity of 6.4 km s^{-1} starting at 3 km depth was assumed. Below the velocity inversion, approximately constant velocity of 6 km s^{-1} is suggested from sonic logs for the updated 1D velocity model (Fig. 1).

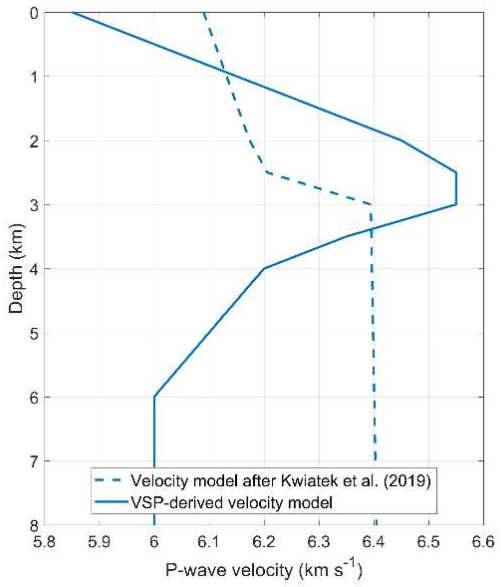

Figure 1. Comparison of 1D velocity model developed from VSP profiling (solid line) and the one used in Kwiatek et al. (2019).

2.4 Earthquake location and relocation

The sub-catalog of 5,456 events was reprocessed applying the new 1D layered velocity model. Thus, the V_P/V_S ratio had to be optimized by a trial-and-error procedure, as discussed in Leonhardt (2020). We found the optimum V_P/V_S by minimizing the cumulative residual errors of all located events while keeping first induced seismic events close to the

injection well *OTN-3*. The optimized V_P/V_S ratio of 1.71 was therefore selected which is similar to that used in Hillers et al. (2020).

The hypocenter locations were estimated using the Equal Differential Time (EDT) method (Zhou, 1994; Font et al., 2004; Lomax, 2005) and the new VSP-derived velocity model. In addition, station corrections were applied. The minimization of travel time residuals:

$$\left|\left|\left(T_j^{th} - T_i^{th}\right) - \left(T_j^{obs} - T_i^{obs}\right)\right|\right|_{L_2} = min, \quad (1)$$

where T^{th} and T^{obs} are all unique pairs (i,j) of theoretical and observed travel times of P- and S-phases, were resolved using the Simplex algorithm (Nelder and Mead, 1965; Lagarias et al., 1998) . A total of 2,958 reprocessed events were absolute located around the injection well *OTN-3* at an epicentral distance of less than 5 km and at depth of 4.5 to 7 km. The hypocenters of these events were included to the reprocessed and published catalog.

To further refine the quality of hypocenter locations, 2,178 from the 2,958 absolute located events with at least 10 P-wave and 4 S-wave picks were selected and the double-difference relocation technique (hypoDD) was applied using the new VSP-derived velocity model (Waldhauser and Ellsworth, 2000). An iterative least-square inversion was used to minimize residuals of observed and predicted travel time differences for event pairs calculated from the existing P- and S-wave picks of the selected catalog data. The residuals were minimized in ten iterations steps. For the last iteration, the maximum threshold for travel time residuals were set to 0.08 s and the maximum distance between the catalog linked event pairs was defined as 170 m. With the hypoDD method 1,986 events were relocated and thus 91 % of the selected 2,178 events. The residuals of the relocations have a root mean square error of 9 ms. The relocation uncertainties were then assessed using a bootstrap technique (Waldhauser and Ellsworth, 2000; Efron, 1982) leading to relative location precision not exceeding ±52 m for 95 % of the catalog.

2.5 Basic source characteristics and statistical properties

Local "Helsinki" magnitude M_{LHEL} has been calculated from ground displacement seismograms integrated from ground velocity records (Uski and Tuppurainen, 1996; further updated by Uski et al. (2015) to smaller events). The magnitude was calculated separately on each station (24 sensors) using vertical component seismograms, and then averaged. The moment magnitudes of all events were estimated from local magnitudes M_{LHEL} using formula from Uski et al. (2015). The seismic moment was recalculated from M_W using formula of Hanks and Kanamori (1979).

The magnitude of completeness M_C as well as the *b*-value were calculated assuming a Gutenberg-Richter (GR) power law: $\log_{10} N = a - bM_C$, where *N* is the cumulative number of earthquakes with magnitudes larger than M_C. Following the Goodness-of-fit method (Wiemer and Wyss, 2000), the magnitude of completeness and the *b*-value were estimated assuming that the GR power law can fit 98 % of the seismic data.

3. Seismic catalog properties

The reprocessed seismic catalog covers the time period between 4th of June and 24th of September 2018. The stimulation was performed during the first 49 days. After shut-in of injection, i.e. after 22nd of July 2018 at 15:52 UTC, further 63 days of the post-stimulation time period were monitored.

Overall, 61,163 earthquakes were detected during and after the stimulation. From the 55,707 events that were detected but not further processed, 52,107 detections occurred during the stimulation whereas another 3,600 detections were monitored after the stimulation. From the 5,456 events that were further processed, 4,510 events were monitored during and 946 events were monitored after the end of stimulation.

3.1 Moment magnitudes

The 55,707 event detections, that were not further located or processed, had moment magnitudes between M_W = -0.95 and M_W = 1.53. The subset of 2,958 events that were absolute located within the target volume around the injection well *OTN-3* with an epicentral distance of less than 5 km and a depth between 4.5 km and 7 km had moment magnitudes between M_W = -0.84 and M_W = 1.87. The 213 post-injection events that were absolute located within the target volume around *OTN-3* showed a minimum moment magnitude of M_W = -0.69. The largest observed magnitude was M_W = 1.54 for the absolute located post-stimulation events. The subset of 1,987 relocated events showed moment magnitudes between M_W = -0.49 and M_W = 1.87. The 70 relocated post-stimulation events had a minimum magnitude of M_W = -0.07.

3.2 Relocated catalog

Figure 2 presents the relocated seismicity which occurred in three spatially separated clusters elongated in southeast (SE) - northwest (NW) direction and centered along the injection well, in good agreement with Kwiatek et al. (2019). Elongation of the clusters in SE-NW direction is sub-parallel to the local maximum horizontal stress S_H^{max} = 110° (Kwiatek et al., 2019). Further details about the relocated seismicity are discussed in Leonhardt et al. (2020).

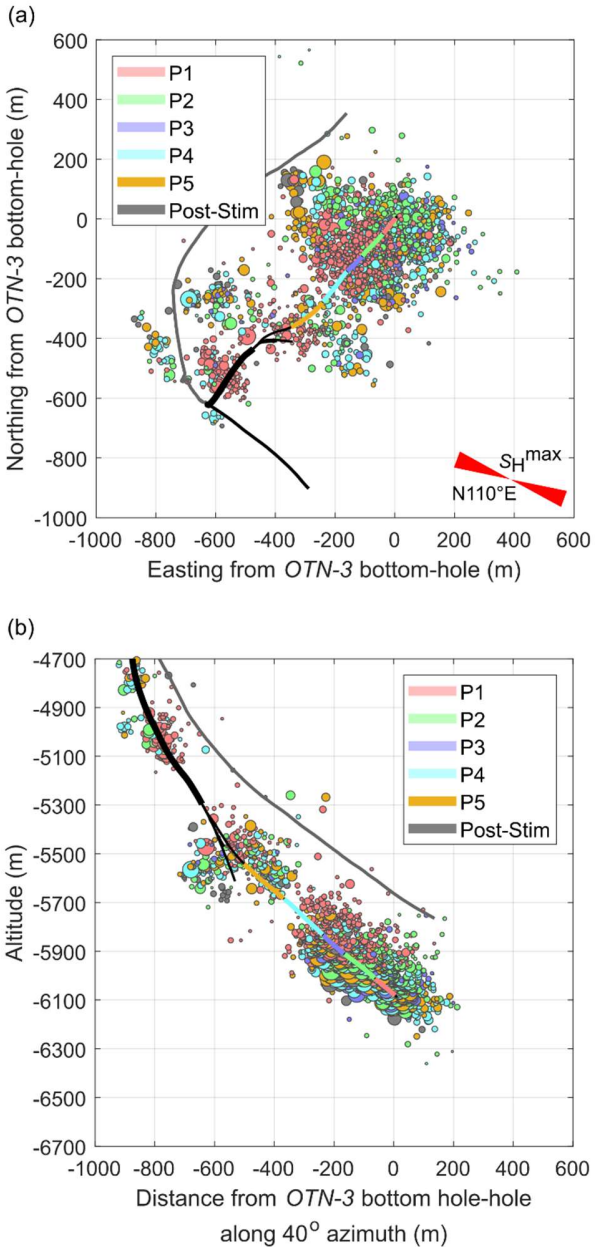

Figure 2. Hypocenters of relocated events. (a) Map view and (b) SW-NE depth section. The hypocenters are color-coded with the stimulation phases (cf. Kwiatek et al., 2019) and size corresponds to moment magnitude. Relocated seismicity that occurred after the stimulation is represented as grey dots. The five injection stages are marked as color bands along the borehole trace from the bottom of the open-hole toward the casing shoe of the injection well *OTN-3* (black). The new *OTN-2* well (grey) was drilled in 2019 to 2020 after the stimulation.

3.3 Spatio-temporal characteristics

Figure 3 shows the development of the seismicity with the horizontal distance from injection well *OTN-3*. This shows quick expansion of seismicity in lateral direction (mostly along SE-NW direction) in first two stimulation phases P1-P2 lasting 20 days (cf. Kwiatek et al., 2019), where the injection rates and injection well head pressures were the highest (cf. Kwiatek et al., 2019; Leonhardt et al., 2020). In following stimulation phases P3-P5, the expansion is slower and the seismicity front reaches approx. 400 m horizontal distance from *OTN-3* well. The post-stimulation phase displays no signatures in propagation with scattered seismicity confined to 400 m horizontal distance from *OTN-3* well.

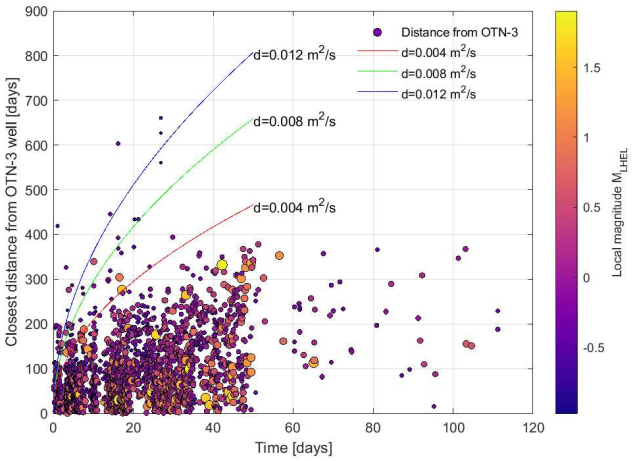

Figure 3. Spatial development of the seismicity with time during *OTN-3* stimulation (until day 49) and in post-stimulation phase (from day 49). For each event, the distance is calculated as a distance between earthquake epicenter (EASTING, NORTHING) and the coordinate of the *OTN-3* well (EASTING, NORTHING) at the depth of earthquake (horizontal distance). The red, blue and green curves represent expected space-time evolution of a fluid pressure perturbation front triggering seismicity assuming that it is solely controlled be scalar fluid pressure diffusion in a homogeneous isotropic medium (e.g. Shapiro et. al., 2020).

Figure 4 presents the dependence between earthquake depth and local magnitude. The figure marks the three distinct clusters of seismicity (cf. Fig. 2) developed during hydraulic stimulation. Largest seismic events as well as the highest level of seismic activity is observed in the lowermost cluster. This is expected due to expected elevated pore fluid pressures in the direct vicinity of injection activities, suggesting the seismic activity, as well as maximum magnitude is pressure-controlled (cf. discussion in Kwiatek et al., 2019; Bentz et al., 2020; Wang et al., 2020a, 2020b).

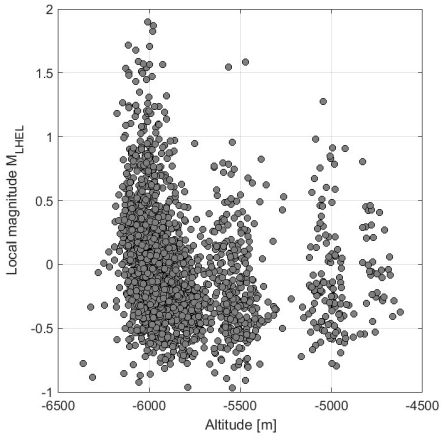

Figure 4. Dependence between earthquake depth (here presented as altitude a.s.l.) and local magnitude.

3.4 Gutenberg-Richter distribution

The catalog combining locations and detections displays b = 1.25 with magnitude of completeness M_C = -1.10 (Figure 5). Above M_{LHEL} 1.5 the statistically significant roll-off is visible which was attributed to either geometrical constraint on pre-existing fracture network or limitation to fault strength (cf. Kwiatek at al., 2019). We note that although the magnitude of completeness of the full catalog is M_C = -1.10, the day-night cycles and associated anthropogenic noises reduces the completeness by approx. 0.2 (cf. Figure 2 in Kwiatek et al. (2019) where day-night cycle is clearly visible).

However, processing of events with M_{LHEL} < -0.7 should be performed with caution. In a pending study (G. Kwiatek – pers. comm.) we note local magnitude estimates of small events with M_{LHEL} < -0.7 are affected by high-frequency noises above 60 Hz (multiple resonance peaks) observed on sensors forming the vertical array in *OTN-2* well. The origin of these noises has been correlated to technological activities at the injection site, with the most likely noise source attributed to the high-performance injection pumps, as the noise seem to be correlation to injection rates. As recordings from *OTN-2* arrays are used to calculate local magnitude of smaller events that are not detected using the sensors close to the surface, and the local magnitude is calculated from integrated ground displacement seismograms which further emphasize the (temporary varying and resonant) noises, we expect significant bias in estimates of M_{LHEL} for M_{LHEL} < -0.7. This may lead to potential problems while analyzing statistical properties of induced seismicity such as magnitude correlations and or inter-event time statistics, to name a few. We suggest M_C = -0.7 as a safe magnitude threshold that is not affected by noises originating from technological activity and day-night cycles. The subject is a topic of pending study (G. Kwiatek – pers. comm.) and this document will be updated accordingly when new information becomes available.

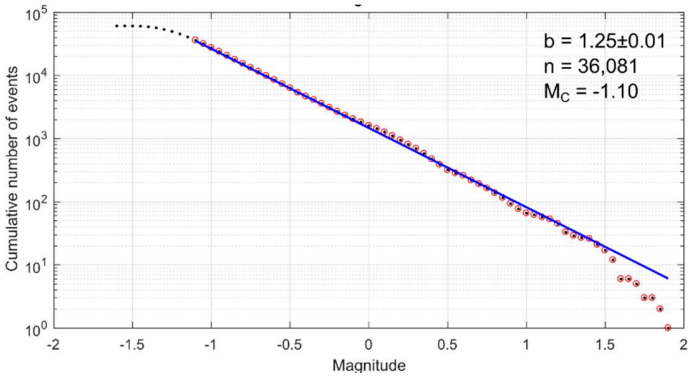

Figure 5. Magnitude-frequency relation for the entire seismic catalog analyzed in Leonhardt et al. (2020).

References

Bentz, S., Kwiatek, G., Martínez-Garzón, P., Bohnhoff, M., and Dresen, G.: Seismic moment evolution during hydraulic stimulations, Geophysical Research Letters, 47, e2019GL086185, https://doi.org/10.1029/2019GL086185, 2019.

Efron, B.: The jackknife, the bootstrap, and other resampling plans, Siam, 1982.

Font, Y., Kao, H., Lallemand, S., Liu, C.-S., and Chiao, L.-Y.: Hypocentre determination offshore of eastern Taiwan using the maximum intersection method, Geophysical Journal International, 158, 655–675, https://doi.org/10.1111/j.1365-246X.2004.02317.x, 2004.

Hanks, T.C. and Kanamori, H.: A moment magnitude scale, Journal of Geophysical Research: Solid Earth, 84, 2348–2350, https://doi.org/10.1029/JB084iB05p02348, 1979.

Hillers, G., Vuorinen, T., Uski, M., Kortström, J., Mäntyniemi, P., Tiira, T., Malin, P., and Saarno, T.: The 2018 geothermal reservoir stimulation in Espoo/Helsinki, Southern Finland: Seismic network anatomy and data features, Seismological Research Letters, 91 (2A), 770–786, https://doi.org/10.1785/0220190253, 2020.

Kwiatek, G., Saarno, T., Ader, T., Bluemle, F., Bohnhoff, M., Chendorain, M., Dresen, G., Heikkinen, P., Kukkonen, I., Leary, P., Leonhardt, M., Malin, P., Martínez-Garzón, P., Passmore, K., Passmore, P., Valenzuela, S., and Wollin, C.: Controlling fluid-induced seismicity during a 6.1-km-deep geothermal stimulation in Finland, Science Advances, 5, eaav7224, https://doi.org/10.1126/sciadv.aav7224, 2019.

Lagarias, J.C., Reeds, J.A., Wright, M.H., and Wright, P.E.: Convergence properties of the Nelder--Mead simplex method in low dimensions, SIAM J. Optim., 9, 112–147, https://doi.org/10.1137/S1052623496303470, 1998.

Leonhardt, M., Kwiatek, G., Martínez-Garzón, P., Bohnhoff, M., Saarno, T., Heikkinen, P., and Dresen, G.: Seismicity during and after stimulation of a 6.1 km deep enhanced geothermal system in Helsinki, Finland, Solid Earth Discuss., https://doi.org/10.5194/se-2020-139, in review, 2020.

Lomax, A.: A reanalysis of the hypocentral location and related observations for the great 1906 California earthquake, Bulletin of the Seismological Society of America, 95, 861–877, https://doi.org/10.1785/0120040141, 2005.

Nelder, J.A. and Mead, R.: A simplex method for function minimization, The Computer Journal, 7, 308–313, https://doi.org/10.1093/comjnl/7.4.308, 1965.

Shapiro, S. A., Rothert, E., Rath, V., and Rindschwentner, J.: Characterization of fluid transport properties of reservoirs using induced microseismicity, Geophysics, 67(1), 212–220, https://doi.org/10.1190/1.1451597, 2020.

Uski, M. and Tuppurainen, A.: A new local magnitude scale for the Finnish seismic network, Tectonophysics, 261, 23–37, https://doi.org/10.1016/0040-1951(96)00054-6, 1996.

Uski, M., Lund, B., and Oinonen, K.: Scaling relations for homogeneous moment based magnitude, in: Evaluating seismic hazard for the Hanhikivi nuclear power plant site. Seismological characteristics of the seismic source areas, attenuation of seismic signal, and probabilistic analysis of seismic hazard, edited by: Saari, J., Lund, B., Malm, M., Mäntyniemi, P., Oinonen, K., Tiira, T., Uski, M., and Vuorinen, T., (Report NE-4459, ÅF-Consult Ltd.), 125 pp., 2015.

Waldhauser, F. and Ellsworth, W.L.: A double-difference earthquake location algorithm: Method and application to the Northern Hayward Fault, California, Bulletin of the Seismological Society of America, 90, 1353–1368, https://doi.org/10.1785/0120000006, 2000.

Wang, L., Kwiatek, G., Rybacki, E., Bohnhoff, M., and Dresen, G.: Injection-induced seismic moment release and lLaboratory fault slip: Implications for fluid-induced seismicity, Geophysical Research Letters, 47, e2020GL089576, https://doi.org/10.1029/2020GL089576, 2020a.

Wang, L., Kwiatek, G., Rybacki, E., Bonnelye, A., Bohnhoff, M., and Dresen, G.: Laboratory study on fluid-induced fault slip behavior: The role of fluid pressurization rate, Geophysical Research Letters, 47, e2019GL086627, https://doi.org/10.1029/2019GL086627, 2020b.

Wiemer, S. and Wyss, M.: Minimum magnitude of completeness in earthquake catalogs: Examples from Alaska, the Western United States & Japan, Bull. Seismol. Soc. Am, 90, 859–869, https://doi.org/10.1785/0119990114, 2000.

Zhou, H.: Rapid three-dimensional hypocentral determination using a master station method, Journal of Geophysical Research: Solid Earth, 99, 15439–15455, https://doi.org/10.1029/94JB00934, 1994.